Multiple Electron Oxidation of Phenols by an Oxo Complex of Ruthenium(IV)

Won K. Seok and Thomas J. Meyer*

Contribution from the Department of Chemistry, The University of North Carolina, Chapel Hill, North Carolina 27599-3290. *Received February 8, 1988*

Abstract: The kinetics of oxidation of phenol and alkylated phenol derivatives by $[(bpy)_2(py)Ru^{IV}(O)]^{2+}$ and $[(bpy)_2(py)Ru^{III}(OH)]^{2+}$ (bpy is 2,2′-bipyridine and py is pyridine) to give the corresponding quinones have been studied in aqueous solution and in acetonitrile. The reactions are first order in both phenol and $Ru^{IV}{=}O^{2+}$ or $Ru^{III}{-}OH^{2+}$. They proceed via a detectable intermediate, which is a Ru(II) complex. ^{18}O isotopic labeling experiments show that transfer of the oxo group from $Ru^{IV}{=}O^{2+}$ to phenol is quantitative. The reactions are facile. With $Ru^{IV}{=}O^{2+}$ as oxidant k (25 °C, CH_3CN) = 1.9 (±0.4) × 10^2 M^{-1} s^{-1}; with $Ru^{III}{-}OH^{2+}$ as oxidant k (25 °C, CH_3CN) = 4.0 (±0.4) × 10 M^{-1} s^{-1}. On the basis of the rate laws, the magnitude of OH/OD and CH/CD kinetic isotope effects, and the ^{18}O labeling results, the most reasonable mechanism for oxidation of phenol by $Ru^{IV}{=}O^{2+}$ appears to be electrophilic attack on the aromatic ring. For $Ru^{III}{-}OH^{2+}$, oxidation appears to occur by CH/H atom transfer in CH_3CN and OH/H atom transfer in water.

There is by now an extensive and growing coordination chemistry of the higher oxidation states of ruthenium and osmium based on stabilization by metal–oxo formation,[1] e.g.

$$[(bpy)_2Os(H_2O)_2]^{2+} \xrightarrow[-4e^-]{-4H^+} [(bpy)_2Os(O)_2]^{2+}$$

Included in this chemistry is a series of polypyridyl complexes of Ru and Os, which have proven to be versatile stoichiometric and/or catalytic oxidants toward a variety of organic or inorganic substrates.[2-8] From the synthetic point of view, the most important feature of the chemistry is that ligand variations can be made that create the basis for a family of MnO_4^--like chemical oxidants where the oxidizing properties can be varied systematically by making variations in the ligands. As part of a larger scheme for developing the potential of this family of oxidants, we have explored the mechanistic details by which a variety of inorganic and organic functional groups are oxidized by the $Ru^{IV}{=}O^{2+}$ oxidants $[(bpy)_2(py)Ru(O)]^{2+}$ and $[(trpy)(bpy)Ru(O)]^{2+}$ (trpy is 2,2′:6′,2″-terpyridine, bpy is 2,2′-bipyridine, and py is pyridine). As shown by the Latimer-type diagram for $[(bpy)_2(py)Ru(H_2O)]^{2+}$ in Scheme I, both the Ru(IV/III) and Ru(III/II) couples are accessible. The $Ru^{IV}{=}O^{2+}$ complex has both 1e and 2e transfer capabilities, with the thermodynamic discrimination between them being slight.

As oxidants the polypyridyl complexes are coordinatively well-defined and chemically stable, and on the basis of their coordinative stabilities, they can be made catalytic by oxidative regeneration of $Ru^{IV}{=}O^{2+}$. The coordinative stability of the complexes, the ease with which they lend themselves to kinetic studies, the availability of the ^{18}O-labeled oxidant, and the appearance of stable intermediates also make them ideal for mechanistic studies. We present here the results of a detailed mechanistic study on the net 4e oxidation of phenol and phenol derivatives by $[(bpy)_2(py)Ru(O)]^{2+}$. Part of this work has appeared in a preliminary communication.[9]

Because of their highly functionalized nature, quinones, which are products of phenolic oxidation, have considerable potential as intermediates in the synthesis of complex organic compounds.[10] This oxidation chemistry has been reviewed,[11] and the results of phenolic oxidation by oxidants such as $Fe(CN)_6^{3-}$, $FeCl_3$, $H_2O_2/RuCl_3$, $Pb(OAc)_4$, MnO_4^-, PbO_2, H_2O_2, peracids, $S_2O_8^-$, O_2, halogens, R_2NO, and Cr(VI) have been reported.[12] The most common oxidation pathway involves initial loss of 1e followed by H^+ loss to give the intermediate phenoxy radical,[13] followed by subsequent oxidation or coupling (eq 1). More complex redox

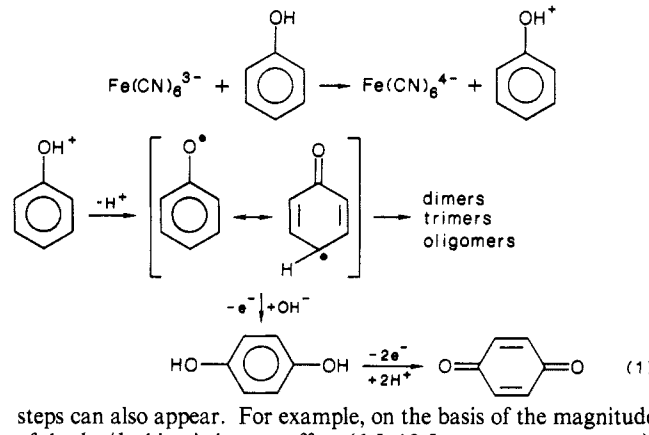

(1)

steps can also appear. For example, on the basis of the magnitude of the k_H/k_D kinetic isotope effect (6.5–10.5 at room temperature),

(1) (a) Griffith, W. P. *Coord. Chem. Rev.* **1970**, *5*, 459. (b) Griffith, W. P.; Rossetti, R. *J. Chem. Soc., Dalton Trans.* **1972**, 1449. (c) Moyer, B. A.; Meyer, T. J. *Inorg. Chem.* **1981**, *20*, 436. (d) Dobson, J. C.; Takeuchi, K. J.; Pipes, D. W.; Geselowitz, D. A.; Meyer, T. J. *Inorg. Chem.* **1986**, *25*, 2537. (e) Holm, R. H. *Chem. Rev.* **1987**, *87*, 1401. (f) Che, C. M.; Leung, W. H. *J. Chem. Soc., Chem. Commun.* **1987**, 1376. (g) Marmion, M. E.; Takeuchi, K. J. *J. Am. Chem. Soc.* **1988**, *110*, 1472.

(2) Meyer, T. J. *J. Electrochem. Soc.* **1984**, *131*, 221c.

(3) Dobson, J. C.; Seok, W. K.; Meyer, T. J. *Inorg. Chem.* **1986**, *25*, 1513.

(4) (a) Roecker, L.; Meyer, T. J. *J. Am. Chem. Soc.* **1986**, *108*, 4066. (b) Roecker, L.; Meyer, T. J. *J. Am. Chem. Soc.* **1987**, *109*, 746.

(5) (a) Moyer, B. A.; Thompson, M. S.; Meyer, T. J. *J. Am. Chem. Soc.* **1980**, *102*, 2310. (b) Thompson, M. S.; De Giovani, W. F.; Moyer, B. A.; Meyer, T. J. *J. Org. Chem.* **1984**, *25*, 4972.

(6) (a) Thompson, M. S.; Meyer, T. J. *J. Am. Chem. Soc.* **1982**, *104*, 4106. (b) Thompson, M. S.; Meyer, T. J. *J. Am. Chem. Soc.* **1982**, *104*, 5070.

(7) (a) Moyer, B. A.; Sipe, B. K.; Meyer, T. J. *Inorg. Chem.* **1981**, *20*, 1475. (b) Roecker, L.; Dobson, J. C.; Vining, W. J.; Meyer, T. J. *Inorg. Chem.* **1987**, *26*, 779.

(8) (a) Che, C. M.; Wong, K. Y.; Mak, T. C. W. *J. Chem. Soc., Chem. Commun.* **1985**, 546. (b) Che, C. M.; Nam, W. W. *J. Am. Chem. Soc.* **1986**, *108*, 4066. (c) Gilbert, J. A.; Roecker, L.; Meyer, T. J. *Inorg. Chem.* **1987**, *26*, 1126. (d) Marmion, M. E.; Takeuchi, K. J. *J. Chem. Soc., Chem. Commun.* **1987**, 1396.

(9) Seok, W. K.; Dobson, J. C.; Meyer, T. J. *Inorg. Chem.* **1988**, *27*, 3.

(10) Evans, D. A.; Hart, D. J.; Koelsch, D. A.; Cain, P. A. *Pure Appl. Chem.* **1979**, *51*, 1285.

(11) (a) Musso, H. *Angew. Chem.* **1963**, *75*, 965. (b) Heusler, K.; Kalvoda, J. *Angew. Chem.* **1964**, *76*, 518. (c) Patai, S. *The Chemistry of Quinoid Compounds*; Wiley: New York, 1974. (d) Posner, G. H. *Angew Chem., Int. Ed. Engl.* **1978**, *17*, 487. (e) Barton, D. H. R.; Brewster, A. G.; Ley, S. V.; Read, C. M.; Rosenfeld, M. N. *J. Chem. Soc., Perkin. Trans. 1* **1981**, 1473.

(12) (a) Patai, S. *The Chemistry of The Hydroxyl* Group; Interscience: New York, 1971. (b) Stoddart, J. F. *Comprehensive Organic Chemistry*; Pergamon: London, 1981; Vol. 1. (c) Lee, D. G.; Sebastian, C. F. *Can. J. Chem.* **1981**, *59*, 2776, 2780. (d) Ito, S.; Aihara, K.; Matsumoto, M. *Tetrahedron* **1983**, 5249. (e) Cornejo, J. J.; Larson, K. R.; Mendenhall, G. D. *J. Org. Chem.* **1985**, *50*, 5382. (f) Ngo, M.; Larson, K. R.; Mendenhall, G. D. *J. Org. Chem.* **1986**, *51*, 5390.

(13) Haynes, C. G.; Turner, A. H.; Waters, W. A. *J. Chem. Soc.* **1956**, 2823.

0002-7863/88/1510-7358$01.50/0

Scheme I[a]

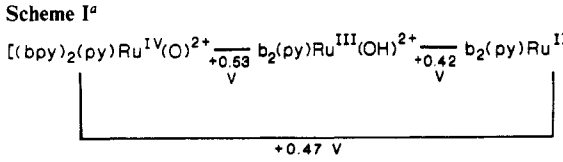

[a] T = 25 °C; I = 0.1 M, pH 7; potential values are vs SCE; b is 2,2′-bipyridine.

H atom transfer has been invoked in the oxidation of phenols by alkoxy radicals.[14]

$$RO^{\bullet} + PhOH \rightarrow ROH + PhO^{\bullet}$$

The primary reason for our interest in the $Ru^{IV}{=}O^{2+}$/Ru^{III}—OH^{2+}/Ru^{II}—OH_2^{2+} redox couples in the context of phenolic oxidation was to establish the mechanism or mechanisms of oxidation. Earlier work has shown that a variety of oxidative pathways are available to the Ru-based oxidants. They include (1) 2e O atom transfer to a reductant,[7] (2) 2e hydride transfer from a reductant,[4b] and (3) 1e pathways involving either H atom transfer[8c] or simple outer-sphere electron transfer from a reductant.

Experimental Section

Materials. Phenol from the Aldrich Chemical Co. was recrystallized twice from petroleum ether. Phenol-d_6, 98 atom %, obtained from Aldrich, was used without purification. Deuterium oxide (Aldrich Gold Label), 99.8%, was used as received. House-distilled water was additionally purified by distillation from alkaline permanganate or by passing through a Millipure water system. Acetonitrile was used either as obtained from Burdick & Jackson Laboratories (water content is 0.002–0.008%) or by distillation from P_2O_5 under an argon atmosphere. All the other phenols, *o*-cresol, *m*-cresol, *p*-cresol, *p*-phenylphenol, *p*-*tert*-butylphenol, *p*-isopropylphenol, 2,6-dimethylphenol, 3,5-dimethylphenol, and 2,3,6-trimethylphenol, were obtained from the Aldrich and purified by standard techniques.[15] ^{18}O-labeled water (isotopic purity >97.1%) was purchased from Isotec, Inc. Sodium phosphate, monobasic monohydrate, $NaH_2PO_4{\cdot}H_2O$, sodium phosphate, dibasic heptahydrate, $Na_2HPO_4{\cdot}7H_2O$, sodium phosphate tribasic, Na_3PO_4, sulfuric acid, H_2SO_4, sodium perchlorate, $NaClO_4{\cdot}xH_2O$, and perchloric acid, $HClO_4$, were all used without further purification in the preparation of buffer solutions. Ionic strength was maintained with the use of sodium sulfate, Na_2SO_4, which had been recrystallized once from distilled water. All other materials were obtained from commercial sources and used as received.

Preparations. $[Ru(bpy)_2(CO_3)]{\cdot}2H_2O$, $[Ru(bpy)_2(py)(OH_2)](ClO_4)_2$, $[Ru(bpy)_2(py)(^{18}OH_2)](ClO_4)_2$, $[Ru(bpy)_2(py)(^{18}O)](ClO_4)_2$, and $[Ru(bpy)_2(py)(O)](ClO_4)_2$ were prepared by previously reported procedures.[7a]

Quinone Complex 1. The quinone complex **1** was prepared by first dissolving $[Ru(bpy)_2(CO_3)]{\cdot}2H_2O$ (64 mg) in a minimum amount of 2 M $HClO_4$. A 2 mol equiv of $(NH_4)_2[Ce(NO_3)_6]$ (G. F. Smith) in 2 M $HClO_4$ was added to the resulting solution. *p*-*tert*-Butylphenol (15 mg)

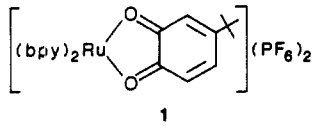

1

was added to this solution, which immediately turned bluish green. The product was placed on a column, which was of 2-cm inner diameter and packed with 20 cm^3 of alumina (Fisher A-540), and eluted by acetonitrile. One drop of an aqueous solution saturated in NH_4PF_6 was added to the first fraction eluted (~2 mL), which gave a green precipitate. The product was collected by filtration, washed with water, and vacuum dried; yield 90%. Anal. Calcd for $C_{30}H_{28}N_4O_2F_{12}P_2Ru$: C, 41.51; H, 3.23; N, 6.46. Found: C, 41.35; H, 3.13; N, 6.12.

Attempts to prepare the monodentate quinone complex **2** by solvent displacement from the intermediate $[(bpy)_2(py)Ru(Me_2CO)]^{2+}$ were successful. Even at relatively high concentrations of added quinone (1 M), there was no evidence for the expected blue color of the bound quinone complex.

Instrumentation. Routine UV–vis spectra were recorded on a Hewlett-Packard 8450A diode array spectrophotometer. IR spectra were

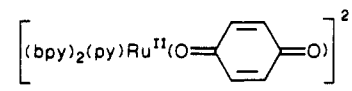

2

obtained on a Nicolet Model 20DX FTIR spectrophotometer either as Nujol mulls or in solutions using NaCl plates. Elementary analyses were obtained from Galbraith Laboratories, Knoxville, TN. ^1H NMR spectra were recorded on an IBM AC 200 spectrophotometer with CD_3CN as solvent and referenced to tetramethylsilane (TMS). Variable-temperature studies were carried out by using a Varian variable-temperature accessory calibrated with methanol by the Van Geet method.[16] Stopped-flow measurements were carried out on two separate systems. Early measurements were performed on an Aminco–Morrow stopped-flow apparatus attached to a Beckman DU monochromator, details of which are given elsewhere.[17] The absorbance–time traces were analyzed by use of a Commodore PET computer Model 4032, which utilizes locally written programs. Later experiments were carried out on a Hi-Tech SF-51 stopped-flow apparatus interfaced to a Zenith 158 microcomputer by using the On Line Instrument Systems (OLIS) stopped-flow program. Fits of the data to kinetic equations were performed on the Zenith 158 microcomputer with OLIS software. Temperature was maintained to ±0.1 °C by a Brinkman Lauda K-2/RD water bath.

Kinetic Measurements. Rate data for oxidations involving $[(bpy)_2(py)Ru(O)]^{2+}$ utilized as the ClO_4^- salt were collected by following the absorbance increase at 675 nm, which is a wavelength of maximum absorbance for the formation of an initial intermediate. Although other wavelengths were accessible, kinetic studies at 675 nm were convenient since they allowed for the direct observation of the appearance and subsequent disappearance of the intermediate. The reactions were carried out under pseudo-first-order conditions in phenol. Pseudo-first-order rate constants were calculated from the slopes of plots of ln $(A_\infty - A_t)$ vs t according to the relation

$$\ln (A_\infty - A_t) = -kt + \ln (A_\infty - A_0)$$

A_∞ is the final absorbance, A_0 is the initial abssorbance, A_t is the absorbance measured at time t, and k is the pseudo-first-order rate constant. The plots were linear for at least 4 half-lives. The pH was controlled with phosphate buffers at constant ionic strength. The rate constants were found to be independent of the buffer concentration. In experiments where $[(bpy)_2(py)Ru^{III}(OH)]^{2+}$ was the oxidant, it was generated in situ by mixing $[(bpy)_2(py)Ru(O)]^{2+}$ with an excess of $[(bpy)_2(py)Ru(OH)_2]$.[18] The kinetic analysis and reaction conditions were the same as described for $[(bpy)_2(py)Ru^{IV}{=}O]^{2+}$ as the oxidant.

Results

Stoichiometry and Product Analysis. In the oxidation of phenol by $[(bpy)_2(py)Ru^{IV}(O)]^{2+}$ in CH_3CN the final metal complex product is $[(bpy)_2(py)Ru^{II}(CH_3CN)]^{2+}$ for which ϵ = 8000 M^{-1} cm^{-1} at λ_{max} = 440 nm. The results of a spectrophotometric titration showed that $[(bpy)_2(py)Ru^{IV}(O)]^{2+}$ was converted quantitatively into $[(bpy)_2(py)Ru^{II}(CH_3CN)]^{2+}$ upon addition of $^1/_2$ mol equiv of phenol. The stoichiometry with regard to the organic oxidation product was established by ^1H NMR and FTIR in the ν(C=O) stretching region. In Figure 1 is shown a ^1H NMR spectrum obtained after allowing 1.1 mg of phenol (11.7 mM) to react with 16.6 mg of $[(bpy)_2(py)Ru(O)]^{2+}$ (23.5 mM) in 1 mL of CD_3CN. Analysis of the resulting spectrum clearly shows the presence of *p*-benzoquinone, *o*-benzoquinone, and the acetonitrile complex $[(bpy)(py)Ru(NCCD_3)]^{2+}$. The stoichiometry in eq 2a was established by integration. The stoichiometry and product distribution for the oxidation of phenol by $[(bpy)_2(py)Ru^{III}$—$OH]^{2+}$ was also established by ^1H NMR (eq 2b). The products of oxidation of the other phenol derivatives by $[(bpy)_2(py)Ru(O)]^{2+}$ were also determined by ^1H NMR and FTIR in the ν(C=O) stretching region. The results are given in Table I.

Mechanistic Studies. In Figure 2 are shown the spectral changes that occur with time in CH_3CN in a solution that was initially 2.2 mM in phenol and 0.046 mM in $[(bpy)_2(py)Ru(O)]^{2+}$. Similar spectral changes were observed for all of the phenols listed in Table I. After mixing, the reactions occur in a stepwise fashion via an

(14) Ingold, K. U. *Can. J. Chem.* **1963**, *41*, 2806.
(15) Perrin, L. G.; Armarego, W. L. F.; Perrin, D. R. *Purification of Laboratory Chemicals*; Pergamon: New York, 1980.
(16) Van Geet, A. L. *Anal. Chem.* **1968**, *40*, 2227.
(17) Cramer, J. L. Ph.D. Dissertation, University of North Carolina, Chapel Hill, NC, 1975.
(18) Binstead, R. A.; Meyer, T. J. *J. Am. Chem. Soc.* **1987**, *109*, 3287.

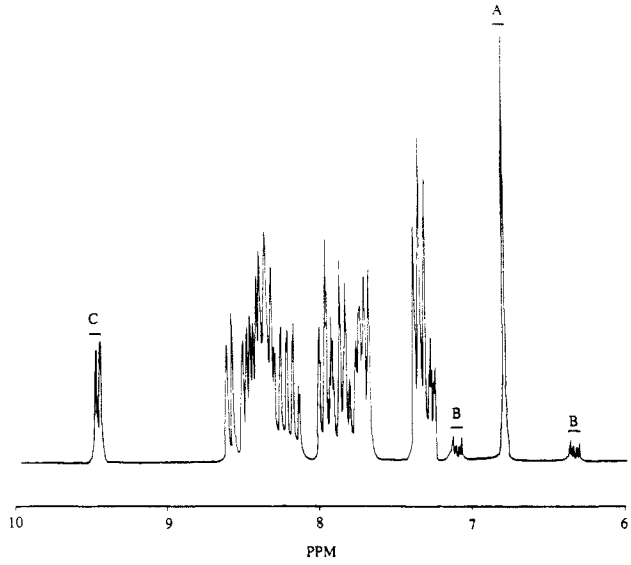

Figure 1. ^1H NMR spectrum of a reaction mixture, which contained initially phenol (11.7 mM) and $[(bpy)_2(py)Ru^{IV}(O)]^{2+}$ (23.5 mM) in 1 mL of CD_3CN at 25 °C. The resonance labeled A arises from *p*-benzoquinone, the resonance B, from *o*-benzoquinone, and that labeled C, from the 6′-position of the bpy ligands. The labeling scheme for the 6′-protons is explained in the text.

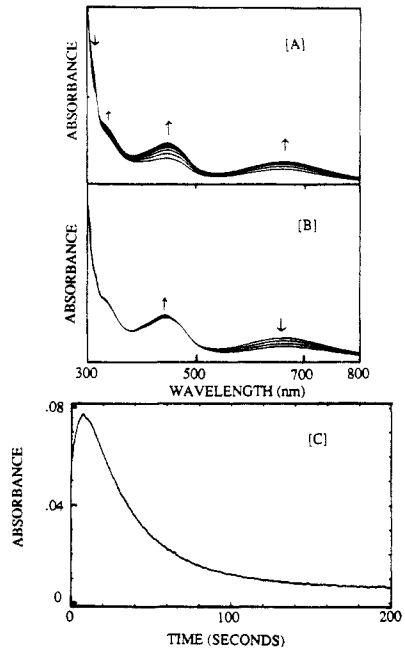

Figure 2. Successive spectral changes observed during the oxidation of phenol (initially 2.2 mM) by $[(bpy)_2(py)Ru(O)]^{2+}$ (initially 0.046 mM) in CH_3CN: (A) the first stage of the reaction showing the absorbance increase at 675 nm every 2 s; (B) the second stage showing the decrease in absorbance at 675 nm every 5 s; (C) the absorbance change vs time at 675 nm.

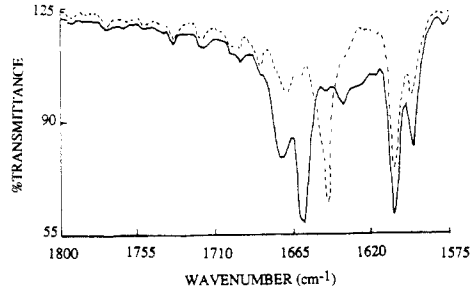

Figure 3. FTIR spectra in CD_3CN of the solutions that result from the oxidation of phenol (9.6 mM) by $[(bpy)_2(py)Ru(^{16}O)]^{2+}$ (—, 19.2 mM) and $[(bpy)_2(py)Ru(^{18}O)]^{2+}$ (---, 19.2 mM).

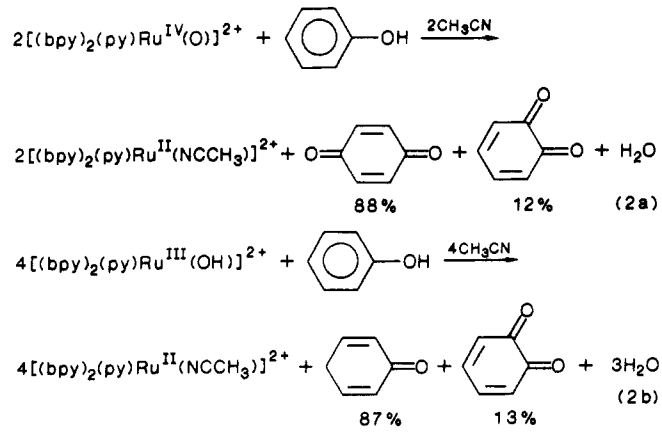

intermediate having λ_{max} = 675 nm, which forms in an initial, rapid step and subsequently undergoes solvolysis to give $[(bpy)_2(py)Ru(NCCH_3)]^{2+}$. The absorbance increase at 675 nm at the end of the first stage of the two-step process is given in Table II for solutions containing initially phenol (2.13 mM) and either $[(bpy)_2(py)Ru(O)]^{2+}$ (0.07 mM) or $[(bpy)_2(py)Ru(OH)]^{2+}$ (0.07 mM) as a function of solvent and pH in water. The notable features in the data are the decreases in ΔA (at 675 nm) above pH 7.01 for $[(bpy)_2(py)Ru(O)]^{2+}$ and, in general, for $[(bpy)_2(py)Ru(OH)]^{2+}$ as oxidant. An ^{18}O tracer study was carried out by using ^{18}O-labeled $[(bpy)_2(py)Ru(O)]^{2+}$ in order to establish the source of the oxygen atom that appears in the benzoquinone products. Figure 3 shows the results of two independent experiments in which $[(bpy)_2(py)Ru(^{18}O)]^{2+}$ (19.2 mM, 85% ^{18}O) and $[(bpy)_2(py)Ru(^{16}O)]^{2+}$ at the same concentration were allowed to react with phenol in CD_3CN. ^{18}O transfer was shown to be quantitative within experimental error by integrating the peak areas for the $\nu(C{=}{}^{16}O)$ = 1660 cm^{-1} and $\nu(C{=}{}^{18}O)$ = 1646 cm^{-1} bands of the dominant (>80%) *p*-benzoquinone product. In some of the quinone products, two $\nu(C{=}O)$ stretching frequencies are observed due to lowered symmetries, intramolecular vibrational coupling, or steric or electronic effects.[19]

The course of the stepwise reaction was also studied by variable-temperature ^1H NMR. The spectra of a reaction mixture initially 19.2 mM in $[(bpy)_2(py)Ru(O)]^{2+}$ and 9.6 mM in phenol in CD_3CN obtained at various temperatures are shown in Figure 4. As alluded to in the caption for Figure 1, in complexes of the type $[(bpy)_2(py)Ru(L)]^{2+}$ (L = H_2O, DMSO, CH_3CN, ...), the chemical shift of one of the 6′-protons, $6'_1$, of the bipyridine rings, which is oriented along the Ru–L bond axis, is shifted upfield because of its presence in the shielding region of the pyridine ring currents. The primed notation refers to the two protons in the 6-positions of the bipyridyl ligands, which in the *cis*-bpy configuration are trans to one another.[20a] The second of the 6′-protons, $6'_2$, is nearest to the ligand L, and its chemical shift is sensitive to the nature of L. Because the $6'_2$-proton is out of the pyridine ring currents, it is shifted downfield. Under high resolution the $6'_2$-resonance provides a very sensitive diagnostic tool for detecting changes in L at the Ru–L coordination site. At −10 °C the $6'_2$-resonance for $[(bpy)_2(py)Ru^{II}(OH_2)]^{2+}$ at 9.2 ppm is somewhat broadened, perhaps because of exchange with $[(bpy)_2(py)Ru^{IV}(O)]^{2+}$, which is paramagnetic[20b] and incompletely reduced at this stage of the reaction. In the −10 °C spectrum, resonances of low intensity appear for $[(bpy)_2(py)Ru^{II}(NCCD_3)]^{2+}$ at 9.42 ppm and an additional peak at 9.12 ppm for the intermediate. Resonances at 6.26 and 6.68 ppm also appear, which are associated with the intermediate. When the temperature was increased to 0 °C in the probe, the 6′-proton and 6.26 and 6.68 ppm protons for the intermediate slowly decrease with a concomitant increase in the

(19) (a) Yates, P.; Ardao, M. I.; Fieser, L. F. *J. Am. Chem. Soc.* **1956**, *78*, 650. (b) Bagli, J. F. *J. Phys. Chem.* **1961**, *65*, 1052. (c) Bagli, J. F. *J. Am. Chem. Soc.* **1962**, *84*, 177.

(20) (a) Lytle, H. E.; Petrosky, L. M.; Carlson, L. R. *Anal. Chim. Acta* **1971**, *57*, 239. (b) Dobson, J. C.; Helms, J. H.; Hatfield, W. E.; Meyer, T. J., submitted for publication.

Table I. Products of the Oxidation of Phenol and Phenol Derivatives by $[(bpy)_2(py)Ru^{IV}{=}O]^{2+}$ in CD_3CN

entry	phenol	benzoquinone[a] products (distribution ratio %) ortho	para	spectral data: ^1H NMR[b] δ_H	FTIR $\nu_{C=O}$, cm^{-1}	UV-vis[c] λ_{max}, nm
1	phenol	12	88	6.3–7.0	1660, 1672	675 (9.9×10^2)
2	*p-tert*-butylphenol	100		6.2–6.9	1668	725 (1.1×10^3)
3	*p*-phenylphenol	100		6.1–6.6	1666	780 (7.6×10^2)
4	*o*-cresol	32	68	6.3–7.0	1662	650 (1.3×10^3)
5	*p*-cresol	100		6.0–7.0	1666	725 (5.6×10^2)
6	*o*-isopropylphenol	38	62	6.2–7.0	1660	650 (1.6×10^3)
7	2,6-dimethylphenol		100	6.5	1655	640 (9.6×10^2)
8	3,5-dimethylphenol	14	86	6.4–6.7	1654	650 (3.0×10^2)
9	2,3-dimethylphenol	11	89	5.9–7.0	1656	625 (1.0×10^3)
10	2,3,6-trimethylphenol		100	7.2	1648	600 (7.2×10^2)

[a] The reactions are quantitative within experimental error. [b] Chemical shifts for the ring protons. Integrations were used to calculate product ratios. [c] Shown in parentheses are ϵ_{max} values (M^{-1} cm^{-1}) for the Ru–quinone intermediates at the maximum wavelength indicated, assuming that the reactions were complete.

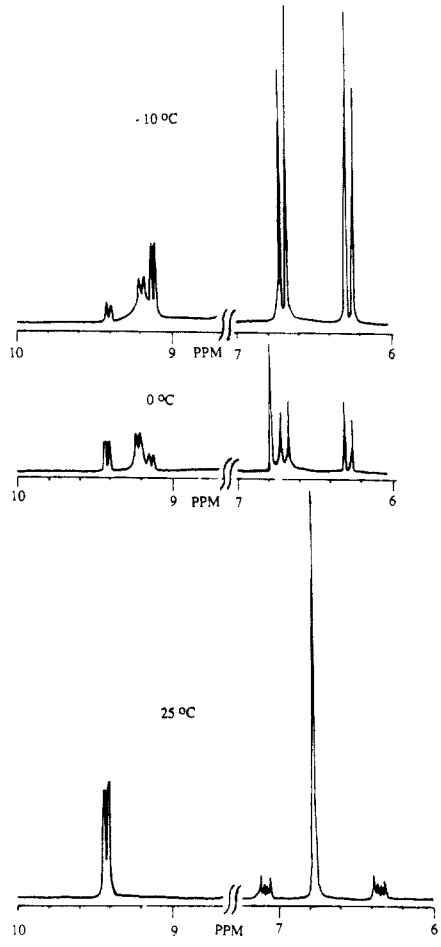

Figure 4. ^1H NMR spectra of a reaction mixture containing initially phenol (9.6 mM) and $[(bpy)_2(py)Ru(O)]^{2+}$ (19.2 mM) in CD_3CN at −10, 0, and +25 °C. Each peak is explained in the text.

$6'_2$-resonance for $[(bpy)_2(py)Ru^{II}(NCCD_3)]^{2+}$. At 25 °C, only resonances for $[(bpy)_2(py)Ru^{II}(NCCD_3)]^{2+}$ were detected in the bipyridine region. The peaks at 6.26 and 6.68 ppm for the intermediate were converted into a single resonance at 6.77 ppm for *p*-benzoquinone.

The nature of the intermediate can be deduced from the ^1H NMR and FTIR data. The ^1H resonances at 6.26 and 6.68 ppm, which have an AB splitting pattern with $J = 10$ Hz, are consistent with either 2e, $[(bpy)_2(py)Ru^{II}(p\text{-}HOC_6H_4OH)]^{2+}$, or 4e products, **2**. Low-temperature IR spectra show the appearance of carbonyl stretching frequencies at 1647 and 1652 cm^{-1} consistent with the bound quinone complex as the greenish blue intermediate. Consistent with this assignment are the properties of the chelated quinone complex **1**. It was prepared by the reaction between $[(bpy)_2Ru^{IV}(O)(OH_2)]^{2+}$ and *p-tert*-butylphenol in 2 M $HClO_4$. The UV–vis spectrum of the complex containing the chelated quinone in CH_3CN (Figure 5) is at least qualitatively consistent with that of the intermediate.

Table II. Absorbance Increase at 675 nm (ΔA) in the Initial Stage of the Oxidation of Phenol by $[(bpy)_2(py)Ru^{IV}{=}O]^{2+}$ or $[(bpy)_2(py)Ru^{III}{-}OH]^{2+}$ at 25 °C ($\mu = 0.1$ M)[a]

oxidant	solvent or pH in H_2O	ΔA
$[(bpy)_2(py)Ru^{IV}{=}O]^{2+}$	1.30	0.066
$[(bpy)_2(py)Ru^{IV}{=}O]^{2+}$	2.40	0.065
$[(bpy)_2(py)Ru^{IV}{=}O]^{2+}$	4.42	0.066
$[(bpy)_2(py)Ru^{IV}{=}O]^{2+}$	5.62	0.070
$[(bpy)_2(py)Ru^{IV}{=}O]^{2+}$	7.01	0.062
$[(bpy)_2(py)Ru^{IV}{=}O]^{2+}$	7.62	0.033
$[(bpy)_2(py)Ru^{IV}{=}O]^{2+}$	8.40	0.017
$[(bpy)_2(py)Ru^{IV}{=}O]^{2+}$	9.06	0.007
$[(bpy)_2(py)Ru^{IV}{=}O]^{2+}$	CH_3CN	0.069
$[(bpy)_2(py)Ru^{III}OH]^{2+}$	7.01	0.016
$[(bpy)_2(py)Ru^{III}OH]^{2+}$	CH_3CN	0.039

[a] The initial concentrations of phenol, $[(bpy)_2(py)Ru(O)]^{2+}$, and $[(bpy)_2(py)Ru(OH)]^{2+}$ were 2.13, 0.07, and 0.07 mM, respectively.

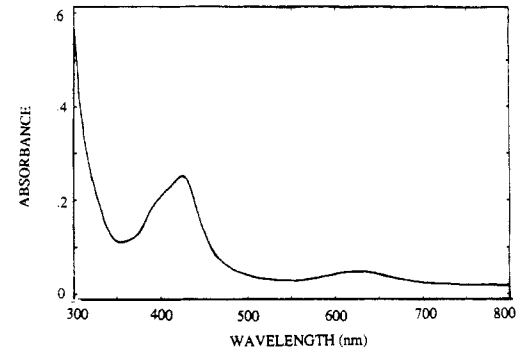

Figure 5. UV–vis spectrum of **1** (0.6 mM), which has $\lambda_{max} = 625$ nm ($\epsilon_{max} = 400$ M^{-1} cm^{-1}) in CH_3CN.

Kinetics

In CH_3CN. From the reaction stoichiometry and the results described above, the oxidation of phenol by $[(bpy)_2(py)Ru(O)]^{2+}$ appears to occur by the series of stepwise reactions in Scheme II. A related series of reactions can be written to account for the appearance of the minority *o*-quinone product.

There is no direct evidence for the 2e intermediate, $[(bpy)_2(py)Ru^{II}(p\text{-}HOC_6H_4OH)]^{2+}$, but direct evidence has been obtained for the quinone complex, which undergoes subsequent solvolysis by CH_3CN. The kinetics of both the initial redox and subsequent solvolysis steps were studied by conventional mixing and stopped-flow experiments. The same results were obtained for the initial redox step by monitoring at 675 or 470 nm. A plot of k_{obs} vs [PhOH] is shown in Figure 6. The bending over of k_{obs} at high

Scheme II

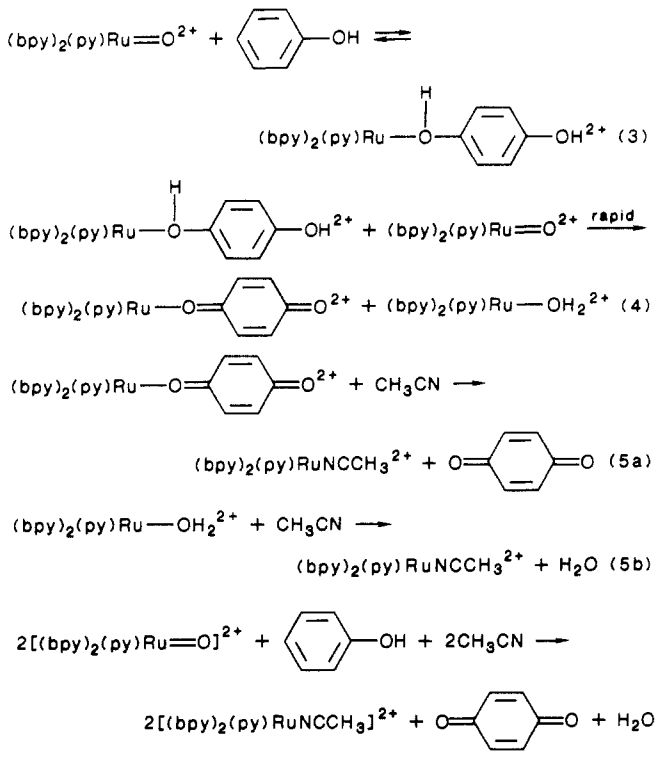

Table III. Rate Constants for the Oxidation of Phenol by $[(bpy)_2(py)Ru(O)]^{2+}$ and by $[(bpy)_2(py)Ru(OH)]^{2+}$ in CH_3CN

oxidant	substrate	T,[a] °C	k,[b,c] M^{-1} s^{-1}
$[(bpy)_2(py)Ru(O)]^{2+}$	C_6H_5OH	14.5	9.3 (±0.4) × 10
$[(bpy)_2(py)Ru(O)]^{2+}$	C_6H_5OH	25.1	1.9 (±0.4) × 10^2
$[(bpy)_2(py)Ru(O)]^{2+}$	C_6H_5OH	27.3	2.3 (±0.3) × 10^2
$[(bpy)_2(py)Ru(O)]^{2+}$	C_6H_5OH	38.5	4.0 (±0.4) × 10^2
$[(bpy)_2(py)Ru(O)]^{2+}$	$C_6H_5OCH_3$	25.1	$<10^{-4}$
$[(bpy)_2(py)Ru(O)]^{2+}$	C_6D_5OH	14.5	3.0 (±0.2) × 10
$[(bpy)_2(py)Ru(O)]^{2+}$	C_6D_5OH	25.1	3.5 (±0.6) × 10
$[(bpy)_2(py)Ru(O)]^{2+}$	C_6D_5OH	27.3	8.5 (±0.8) × 10
$[(bpy)_2(py)Ru(O)]^{2+}$	C_6D_5OH	38.5	1.3 (±0.1) × 10^2
$[(bpy)_2(py)Ru(OH)]^{2+}$	C_6H_5OH	24.8	4.0 (±0.2) × 10
$[(bpy)_2(py)Ru(OH)]^{2+}$	C_6D_5OH	24.8	6.2 (±0.3) × 10

[a] ±0.1 °C. [b] Average of four separate kinetic runs at four different concentrations of phenol. [c] The values cited were calculated as $k_{obs}/2$ for $Ru^{IV}{=}O^{2+}$ and $k_{obs}/4$ for $Ru^{III}{-}OH^{2+}$ on the basis of the reaction stoichiometry in reactions 2a and 2b.

concentrations of phenol has been observed for other substrates.[6,8c,21] The effect is attributable to preassociation prior to the redox step (eq 6).

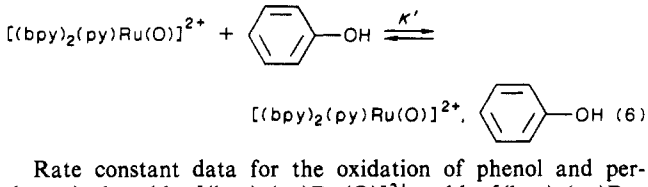

Rate constant data for the oxidation of phenol and perdeuteriophenol by $[(bpy)_2(py)Ru(O)]^{2+}$ and by $[(bpy)_2(py)Ru(OH)]^{2+}$ in CH_3CN are summarized in Table III. In solutions relatively dilute in phenol the reactions are first order in oxidant and first order in phenol (eq 7 and 8). The rate constants for

$$-d[Ru^{IV}{=}O^{2+}]/dt = k_{obs}[Ru^{IV}{=}O^{2+}][PhOH] = dk[Ru^{IV}{=}O^{2+}][PhOH] \quad (7)$$

$$-d[Ru^{III}{-}OH^{2+}]/dt = k_{obs}[Ru^{III}{-}OH^{2+}][PhOH] = 4k[Ru^{III}{-}OH^{2+}][PhOH] \quad (8)$$

the oxidations by $Ru^{III}{-}OH^{2+}$ or $Ru^{IV}{=}O^{2+}$ were unaffected by

(21) Curry, M. E.; Seok, W. K.; Dobson, J. C.; Meyer, T. J., to be submitted for publication.

Table IV. Rate Constants for the Solvolysis of the Ruthenium–Quinone Intermediates at 25.0 (±0.1) °C[a]

substrate	$k(CH_3CN)$, s^{-1} × 10^2	$k(H_2O, \mu = 0.1$ M),[b] s^{-1} × 10^2 pH 2.4	pH 3.4	pH 4.4	pH 5.6	pH 7.0	pH 7.6
phenol	3.8 (±0.3)	4.9	5.6	8.1	11.6	26.0	71.5
p-tert-butylphenol	0.62 (±0.03)					170	
p-phenylphenol	0.49 (±0.05)					290	
o-cresol	0.24 (±0.02)					9.2	
p-cresol	1.2 (±0.1)					350	
o-isobutylphenol	1.4 (±0.1)					4.0	
2,6-dimethylphenol	1.4 (±0.1)					4.2	
3,5-dimethylphenol	1.3 (±0.1)					4.4	
2,3-dimethylphenol	5.5 (±0.5)					20.0	
2,3,6-trimethylphenol	3.7 (±0.4)					10.0	

[a] The solvolysis rates were independent of phenol concentration at each pH. The values were average values for four different determinations. [b] ±5%.

Table V. Rate Constants for the Oxidation of Phenol by $[(bpy)_2(py)Ru(O)]^{2+}$ and by $[(bpy)_2(py)Ru(OH)]^{2+}$ in H_2O (μ = 0.1 M)[a]

oxidant	pH	T, °C	k, M^{-1} s^{-1} × 10^{-2}
$[(bpy)_2(py)Ru(O)]^{2+}$	1.0	24.8	4.4 (±0.2)
$[(bpy)_2(py)Ru(O)]^{2+}$	1.3	24.8	4.2 (±0.2)
$[(bpy)_2(py)Ru(O)]^{2+}$	1.7	24.8	4.1 (±0.3)
$[(bpy)_2(py)Ru(O)]^{2+}$	2.4	24.8	3.3 (±0.1)
$[(bpy)_2(py)Ru(O)]^{2+}$	2.8	24.8	3.4 (±0.2)
$[(bpy)_2(py)Ru(O)]^{2+}$	3.4	24.8	3.7 (±0.2)
$[(bpy)_2(py)Ru(O)]^{2+}$	4.4	24.8	4.1 (±0.2)
$[(bpy)_2(py)Ru(O)]^{2+}$	7.0	10.4	3.6 (±0.3)
$[(bpy)_2(py)Ru(O)]^{2+}$	7.0	24.8	5.6 (±0.5)
$[(bpy)_2(py)Ru(O)]^{2+}$	7.0	32.7	7.6 (±0.6)
$[(bpy)_2(py)Ru(O)]^{2+}$	7.0	40.4	12.5 (±0.7)
$[(bpy)_2(py)Ru(O)]^{2+}$	7.6	24.8	11.0 (±1.3)
$[(bpy)_2(py)Ru(OH)]^{2+}$	7.0	24.8	0.7 (±0.1)

[a] Average of four separate determinations at four different concentrations of phenol. Note footnote *c* of Table III.

argon purging. The rate constants cited in Table III are for the initial redox step. They were calculated from k_{obs} as $k_{obs}/2$ for $Ru^{IV}{=}O^{2+}$ as the oxidant and $k_{obs}/4$ for $Ru^{III}{-}OH^{2+}$ in accordance with reactions 2a and 2b and the experimental rate laws.

Activation parameters for the reactions between $[(bpy)_2(py)Ru(O)]^{2+}$ and C_6H_5OH or C_6D_5OD in CH_3CN were obtained from plots of ln (k/T) vs $1/T$ over the temperature range of 15–40 °C. The results are shown in Table VI. H/D kinetic isotope effects are also listed in Table VI.

Rate constant data were also collected for the solvolysis of the various Ru(II)–quinone intermediates. The results are collected in Table IV. The solvolysis rates were independent of the concentration of added phenol. Activation parameters for the solvolysis of **2** were obtained from plots of ln (k/T) vs $1/T$ over the temperature range of 14–36 °C, which gave $\Delta H^{\ddagger}$ = 14.2 (±0.6) kcal/mol and $\Delta S^{\ddagger}$ = −18 (±2) eu.

In H_2O. The kinetics of formation of the intermediate in the oxidation of phenol by $Ru^{IV}{=}O^{2+}$ were monitored at 675 nm at a series of pH values (Table V). The reactions are also first order in phenol and in $Ru^{IV}{=}O^{2+}$ or $Ru^{III}{-}OH^{2+}$. However, as shown by the data in Table V, k_{obs} is pH dependent for $Ru^{IV}{=}O^{2+}$, increasing both above pH 7 and, more slightly, in acidic solution. Because of experimental limitations, we were unable to extend the kinetic studies above pH 7.6 and were unable to study the pH dependence in detail. The rate enhancement at higher pH may arise because of an enhanced rate of oxidation of phenoxide compared to phenol, which would give the rate law in eq 9 (pK_a = 9.99 for PhOH at 25 °C, μ = 1 M).[22] In water the overall

$$-d[Ru^{IV}{=}O^{2+}]/dt = 2[Ru^{IV}{=}O^{2+}](k[PhOH] + k_{OH^-}[PhO^-]) \quad (9)$$

(22) Biggs, A. I. *J. Chem. Soc.* **1961**, 2572.

Table VI. Summary of Kinetic and Thermodynamic Parameters for the Oxidation of Phenol and Deuteriated Phenol by $[(bpy)_2(py)Ru(O)]^{2+}$ and $[(bpy)_2(py)Ru(OH)]^{2+}$

reaction	medium	k,[a] M^{-1} s^{-1}	$\Delta H^{\ddagger}$, kcal/mol	$\Delta S^{\ddagger}$, eu	k_H/k_D[a]
$Ru^{IV}{=}O^{2+}$ + C_6H_5OH	CH_3CN	1.9 (±0.4) × 10^2	10.3 (±0.6)	−14 (±2)	
$Ru^{IV}{=}O^{2+}$ + C_6D_5OH	CH_3CN	3.5 (±0.6) × 10	10.8 (±1.2)	−14 (±1)	5.5 (±0.2)
$Ru^{IV}{=}O^{2+}$ + C_6H_5OH	H_2O (pH 7)	5.6 (±0.6) × 10^2	6.4 (±1.5)	−24 (±4)	
$Ru^{IV}{=}O^{2+}$ + C_6D_5OH	H_2O (pH 7)	4.8 (±0.4) × 10^2			1.2 (±0.2)
$Ru^{IV}{=}O^{2+}$ + C_6H_5OD	D_2O (pD 7)	1.9 (±0.2) × 10^2			3.5 (±0.5)
$Ru^{III}{-}OH^{2+}$ + C_6H_5OH	CH_3CN	4.0 (±0.4) × 10			
$Ru^{III}{-}OH^{2+}$ + C_6D_5OH	CH_3CN	6.3 (±0.2)			6.3 (±0.4)
$Ru^{III}{-}OH^{2+}$ + C_6H_5OH	H_2O (pH 7)	6.5 (±0.5) × 10			
$Ru^{III}{-}OH^{2+}$ + C_6D_5OH	H_2O (pH 7)	5.5 (±0.5) × 10			1.4 (±0.2)
$Ru^{III}{-}OH^{2+}$ + C_6H_5OD	D_2O (pD 7)	9.5 (±0.2)			7.4 (±0.4)

[a] Average of five determinations at a single concentrations (T = 25 °C).

mechanism of oxidation of phenol remains the same except that the solvolysis step in reaction 5a is replaced by its aqua equivalent.

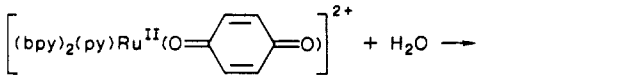

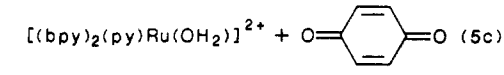

The rate constant for the oxidation of phenol by $[(bpy)_2(py)Ru^{III}(OH)]^{2+}$ at pH 7 is also given in Table V. The value reported is $k_{obs}/4$, consistent with the stoichiometry in reaction 2.

The rate constant for the solvolysis of the ruthenium quinone intermediate for phenol (reaction 5c) is also pH dependent (Table IV). The increase in k_{obs} with pH can be fit to the rate expression in eq 10 where I is **2**, k_1 = 0.065 s^{-1}, and k_2 = 1.8 × 10^4 M^{-1} s^{-1}.

$$-d[I]/dt = k_{obs}[I] = (k_1 + k_2[OH^-])[I] \qquad (10)$$

Activation parameters for the solvolysis of the intermediate at pH 4.5 were calculated from plots of ln (k/T) vs $1/T$, which gave $\Delta H^{\ddagger}$ = 14.7 (±1.4) kcal/mol and $\Delta S^{\ddagger}$ = −11 (±4) eu. At this pH, there are nearly equal contributions from the k_1 and k_2 pathways.

Discussion

The results of simple mixing experiments provide clear evidence for an intermediate in the oxidation of phenol by $[(bpy)_2(py)Ru(O)]^{2+}$, Figure 2. In this work our primary goals were first to establish the mechanism of oxidation of phenol by $[(bpy)_2(py)Ru^{IV}{=}O]^{2+}$ and for comparison by the 1e oxidant $[(bpy)_2(py)Ru^{III}{-}OH]^{2+}$. We also wanted to extend the oxidation chemistry to a series of phenols in order to show the generality of the reaction and to observe the effect of substituents on reactivity.

The reactions are quantitative and involve net 4e changes, e.g.

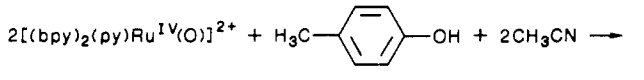

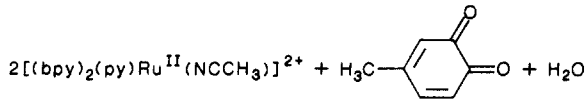

This is in contrast to the results of oxidation by typical 1e oxidants where complex reaction mixtures are often observed arising from radical coupling, e.g., reaction 1.

We have made no attempt to exploit the $Ru^{IV}{=}O^{2+}$-based oxidations synthetically. Previous work has shown that the $Ru^{IV}{=}O^{2+}/Ru^{II}{-}OH_2^{2+}$ couples $[(bpy)_2(py)Ru(O)]^{2+}/[(bpy)_2(py)Ru(OH_2)]^{2+}$ and $[(trpy)(bpy)Ru(O)]^{2+}/[(trpy)(bpy)Ru(OH_2)]^{2+}$ can be utilized as chemical or electrochemical oxidation catalysts toward a variety of organic substrates.[2,5] Their properties as catalytic oxidants are applicable to phenolic oxidations as well.

For phenol itself, and for substituted phenols where the ortho and para positions are available to oxidative attack, a competition exists for the site of oxidation, Table I. The product ratio is 88% *p*-benzoquinone and 12% *o*-benzoquinone for phenol. From the data in Table I, alkyl substitution at either the ortho or para positions blocks oxidation at that position (entries 2, 3, 5, 7, and 10), as expected. At least for methyl groups as substituents, there is no evidence for significant steric effects in determining the product ratios as evidenced by the results in entries 8 and 9, and the regioselectivity may be dictated largely by electronic effects. For example, comparison among entries 1, 4, and 6 suggests that α alkyl substitution does appear to tip the balance in favor of ortho attack.

Mechanism of Oxidation by $Ru^{IV}{=}O^{2+}$ in CH_3CN. The results of the kinetics, ^{18}O-labeling experiments, and the appearance of the reaction intermediate are all consistent with the mechanism in Scheme II for the oxidation of phenol by $[(bpy)_2(py)Ru^{IV}(O)]^{2+}$. The rate constants and activation parameters associated with the individual steps in the scheme are listed in Tables IV and VI. The same pattern of reactions was observed for the phenol derivatives including the appearance and loss of intermediates that absorb in the region 520–760 nm with ϵ_{max} values in the range (1.7–3.7) × 10^3 M^{-1} cm^{-1}. These reactions occur by the same mechanism.

We have obtained no direct evidence for the proposed 2e intermediate, $[(bpy)_2(py)Ru^{II}(p\text{-}HOC_6H_4OH)]^{2+}$. In the ^1H NMR experiment shown in Figure 4, the initial, simultaneous appearance of *both* $[(bpy)_2(py)Ru^{II}{-}OH_2]^{2+}$ and the quinone intermediate is relatively clear in showing that the 4e stage is reached without the buildup of a 2e intermediate. The existence of an intermediate in the reaction is required by the rate law and the 4e-oxidized character of the intermediate quinone complex. The results of the ^{18}O-labeling experiment suggest that O-insertion occurs at the 2e stage.

Even if it were formed, a 2e hydroquinone intermediate would not be expected to build up in solution. The oxidation of free hydroquinone by $[(bpy)_2(py)Ru^{IV}(O)]^{2+}$ in CH_3CN is very rapid, k (25 °C) = 5 × 10^5 M^{-1} s^{-1}.[23] The second redox step in Scheme II (reaction 4) is presumably rapid for the bound hydroquinone as well.

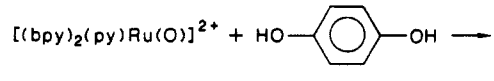

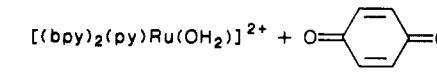

The characterization of the 4e intermediate as a Ru^{II}–quinone complex is consistent with a number of lines of evidence: (1) the IR spectrum in the ν(C=O) region (Figure 3) is consistent with the expected quinoidal structure. (2) Its ^1H NMR spectrum includes an AB splitting pattern involving two protons per site by integration (Figure 4), which is consistent with the asymmetric bound quinone structure. (3) Somewhat related chelated quinone complexes such as **3** have been prepared and characterized.[24] (4)

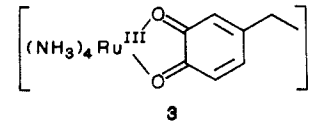

3

(23) McGuire, M. E.; Roecker, L.; Seok, W. K.; Meyer, T. J., to be submitted for publication.

We have been unable to isolate the intermediate because of its lability. We have prepared the related complex **1**, which is stable toward ligand loss because of the chelate effect. The preparation proceeds as in the oxidation of phenol by $[(bpy)_2(py)Ru(O)]^{2+}$ and takes advantage of the labile aqua site in the cis position to form the chelate (eq 11).

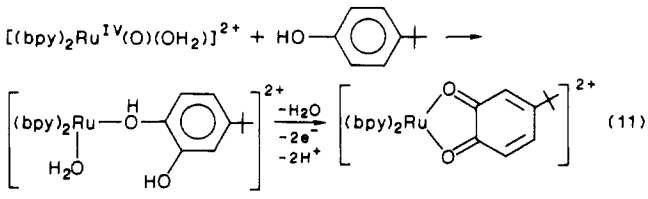

(11)

^1H NMR and UV–vis spectral changes show that once formed the quinone intermediates undergo loss of the quinone ligand by solvolysis (reactions 5a and 5b) on the same time scale as exchange of CH_3CN for H_2O in $[(bpy)_2(py)Ru^{II}(OH_2)]^{2+}$, k (25 °C) = 1.4×10^{-3} s^{-1}. Although the two rates are competitive, loss of quinone can be followed separately by spectral monitoring of the disappearance of the low-energy absorption band at 650–700 nm (Table IV), giving, for example, k (25 °C, CH_3CN) = 3.8×10^{-2} for the quinone complex derived from phenol. For those cases where competitive ortho and para attack must give rise to two intermediates, only single-exponential decays were observed. Apparently, the rate constants for solvolysis are close, and/or one of the products dominates the observed spectral changes.

Mechanism of Oxidation by Ru^{IV}=O^{2+} in H_2O: The Solvolysis Step. The mechanistic pattern for the oxidation of phenol remains the same in water at least up to pH 7. The quinone intermediate appears and is converted into the aqua complex (reaction 5c) with k (25 °C) = 0.26 s^{-1}. The same pattern is maintained for the substituted phenols.

Although there are no obvious trends in the solvolysis rate constants on a case for case basis, rates are accelerated in water compared to those in acetonitrile at room temperature. From the temperature-dependent data for quinone loss in the two solvents, the major difference occurs in the entropies of activation with $\Delta S^{\ddagger}$ = −11 ± 4 (H_2O) and −18 ± 2 (CH_3CN) for the intermediate derived from phenol. In water there is a special rate acceleration for those cases like *p*-cresol where the *o*-quinone is the product, e.g., compound **4**.

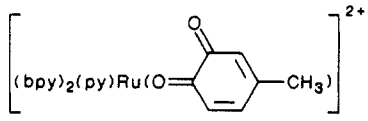

4

The "ortho" effect is not simply steric in origin given the normal rate constant for solvolysis of **5**, for example. It may be related

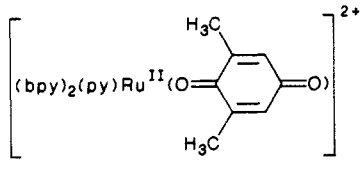

5

to the mechanism for the appearance of the chelated *o*-quinone product with *cis*-$[(bpy)_2Ru(O)(OH_2)]^{2+}$ as oxidant, which is accessible because of the relatively labile aqua group (reaction 11). However, in ^1H NMR experiments, there was no sign of $[(bpy)_2Ru^{II}(NCCH_3)_2]^{2+}$ as a product in the oxidation of the para-substituted phenols by $[(bpy)_2(py)Ru^{IV}(O)]^{2+}$ as oxidant. Pyridine is retained in the coordination sphere during the oxidations, and chelation does not occur.

For loss of quinone in water a "base hydrolysis" pathway appears, which accounts for ~85% of the solvolysis by pH 7.0. The rate constants for the OH^--dependent and -independent paths at 25 °C (μ = 0.1 M) are $k_2 = 1.8 \times 10^4$ M^{-1} s^{-1} and k_1 = 0.065 s^{-1} (eq 10). Since there are no readily dissociable protons in the complex, the base hydrolysis pathway must involve addition of OH^-. One possibility is that the mechanism involves "associative" addition of OH^- to Ru to give a 7-coordinate intermediate or activated complex followed by Ru–O bond breaking. A second would involve OH^- attack at the C atom of the bound quinone O atom followed by O–C bond breaking.

Mechanism of Oxidation by Ru^{III}—OH^{2+}. The stoichiometry of the oxidation of phenol by $[(bpy)_2(py)Ru^{III}(OH)]^{2+}$ in CH_3CN is given by reaction 2b. In water the final metal complex product is $[(bpy)_2(py)Ru^{II}(H_2O)]^{2+}$. Kinetic studies in either solvent show that the reactions are first order in Ru^{III}—OH^{2+} and first order in phenol with a slight rate enhancement at pH 7 compared to that of CH_3CN, Table III. The simple first-order dependence on the two reactants rules out an important role mechanistically for initial disproportionation, followed by oxidation by Ru^{IV}=O^{2+}.

$$2[(bpy)_2(py)Ru^{III}(OH)]^{2+} \rightarrow [(bpy)_2(py)Ru^{IV}(O)]^{2+} + [(bpy)_2(py)RuOH_2]^{2+}$$

This pathway is known to play an important role in the oxidation of alcohols.[6a] It is expected to be unimportant here. The disproportionation reaction is thermodynamically uphill by 0.12 eV, and the rate constants for oxidation by Ru^{III}—OH^{2+} and Ru^{IV}=O^{2+} are within a factor of 10 of each other.

From the data in Table II, the greenish blue intermediate also forms with Ru^{III}—OH^{2+} as oxidant but in CH_3CN, at a level only 50% as high as that for Ru^{IV}=O^{2+} as oxidant. In water at pH 7, the rate of oxidation by Ru^{III}—OH^{2+} is only 8 times slower than that for Ru^{IV}=O^{2+} (Table V), but only 25% of the quinone intermediate appears.

The Ru^{III}—OH^{2+} form of the $[(bpy)_2(py)Ru^{III}(OH)]^{2+}$/$[(bpy)_2(py)Ru^{II}(H_2O)]^{2+}$ couple is a mild oxidant, $E^{\circ\prime}$ = 0.67 V (25 °C, μ = 0.1 M at pH 7 vs NHE). It is constrained to be a 1e oxidant by the nature of the Ru(III/II) couple. With other 1e oxidants, the chemistry of phenol is dominated by initial 1e transfer to give the corresponding phenoxy radical,[25,26] reaction 1. The outer-sphere or radical-cation pathway is well established and is the accepted mechanism for the electrochemical oxidation of phenols.[27]

For Ru^{III}—OH^{2+} as oxidant in CH_3CN, the appearance of a significant C_6H_5OH/C_6D_5OH isotope effect (k_H/k_D = 6.3 at 25 °C, μ = 0.1 M) suggests that the initial redox step may involve C–H/H atom transfer.

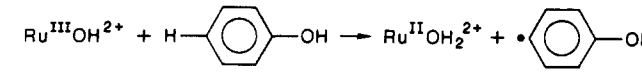

It would be followed by rapid rearrangement of the hydroxylic proton to give the stable form of the phenoxy radical. The

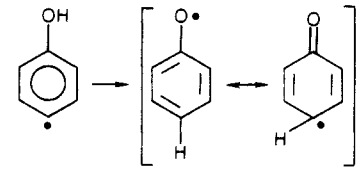

magnitude of the kinetic isotope effect and the suggestion of H atom transfer has precedence in the oxidation of a series of phenols by alkoxy radicals as mentioned in the introduction.[14,25,26]

The appearance of $[(bpy)_2(py)Ru^{II}(p\text{-benzoquinone})]^{2+}$ as an intermediate demands that in a subsequent redox step Ru^{III}—OH^{2+} attack on the phenoxy radical must occur with O–C bond

(24) Pell, S. D.; Salmonsen, R. B.; Abelleira, A.; Clarke, M. J. *Inorg. Chem.* **1984**, *23*, 385.
(25) (a) Masso, H. *Angew. Chem., Int. Ed. Engl.* **1963**, *2*, 723. (b) Scott, A. I. *Quart. Rev., Chem. Soc.* **1965**, *19*, 1. (c) Altwicken, E. R. *Chem. Rev.* **1967**, *67*, 475. (d) Cecil, R.; Littler, J. S. *J. Chem. Soc. B* **1968**, 1420.
(26) (a) Howard, J. A.; Ingold, K. U. *Can. J. Chem.* **1964**, *42*, 2324. (b) Shelton, J. R.; Vincent, D. W. *J. Am. Chem. Soc.* **1964**, *85*, 2433.
(27) Yoshida, K. *Electrooxidation in Organic Synthesis*; Wiley: New York, 1984; 57.

Scheme III[a]

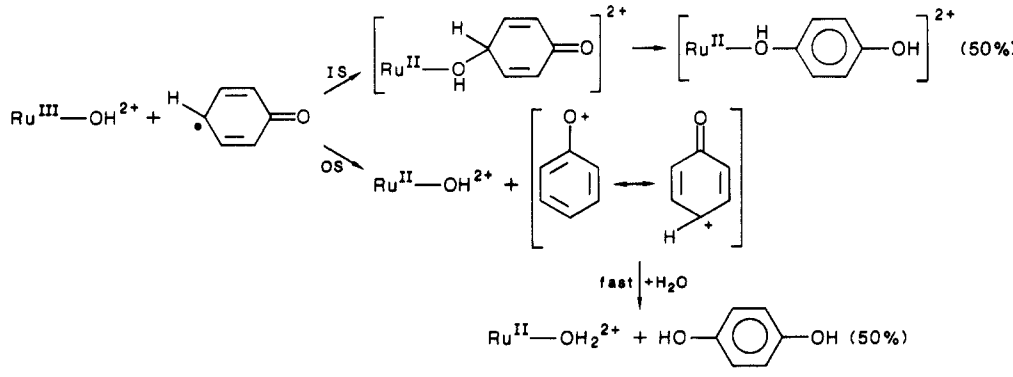

[a] In CH_3CN.

formation. The fact that the yield of the intermediate is ~50% of that for $Ru^{IV}=O^{2+}$ in CH_3CN and ~25% in H_2O suggests that a competition between further oxidation of the phenoxy radical by competing inner-sphere (IS) and outer-sphere (OS) pathways must exist (Scheme III). Once formed, the oxidation of free hydroquinone to quinone is known to be rapid.[23]

Although C–C and C–O ring coupling products are commonly observed for other 1e oxidants,[28] they are not observed here as products. The subsequent oxidation of the phenoxy radicals by Ru^{III}—OH^{2+} must be relatively rapid. The absence of a dependence of k_{obs} on O_2 shows that O_2 is also not involved oxidatively. Even in "dry" acetonitrile, there is sufficient H_2O (>12 mM) to provide the H_2O requirement for the net reaction.

Mechanistic precedence exists for the inner-sphere capture of intermediate phenoxy radicals in the oxidation of phenols to quinones by nitroxide radicals[29] and by Fremy's salt.[30] Mechanistically, these reactions have been suggested to occur by initial oxidation to phenoxy radicals followed by capture by RR'NO hydrolytic hydrolytic loss of RR'NOH to give the quinone.

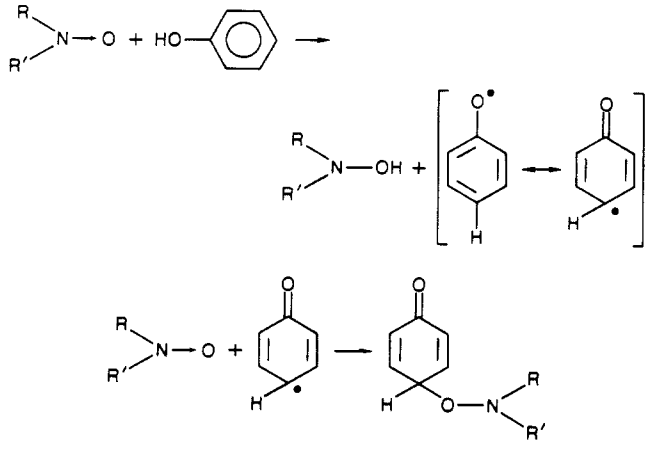

In water the k_{CH}/k_{CD} isotope effect falls to 1.4 at 25 °C (μ = 0.1 M) for C_6H_5OH compared to that for C_6D_5OH, and a large k_{OH}/k_{OD} isotope effect appears. For C_6H_5OH/C_6H_5OD, k_H/k_D = 7.4 ± 0.4 at 25 °C (μ = 0.1 M). The isotope effects suggest that a change in mechanism must occur between H_2O and CH_3CN with a considerable contribution from the O–H bond existing in H_2O.

There are interesting similarities between the oxidations of phenol, H_2O_2,[8c] and $[(bpy)_2(py)Ru^{II}—OH_2]^{2+}$ [18] by Ru^{III}—OH^{2+}. The appearance of large (16.2 and 5.8) OH/OD kinetic isotope effects for the latter two reactions has led to the suggestion that they occur by H atom or "H^+ assisted electron" transfer pathways, e.g.

$$[(bpy)_2(py)Ru^{III}—OH]^{2+} + H_2O_2 \rightarrow [(bpy)_2(py)Ru^{II}—OH_2]^{2+} + HO_2$$

$$[(trpy)(bpy)Ru^{III}—OH]^{2+} + [(bpy)_2(py)Ru^{II}—OH_2]^{2+} \rightarrow [(trpy)(bpy)Ru^{II}—OH_2]^{2+} + [(bpy)_2(py)Ru^{III}—OH]^{2+}$$

All three reactions may occur by closely related mechanisms where the key redox step is H atom transfer from the reductant to the oxidant. Mechanistically, H atom transfer to the oxidant is

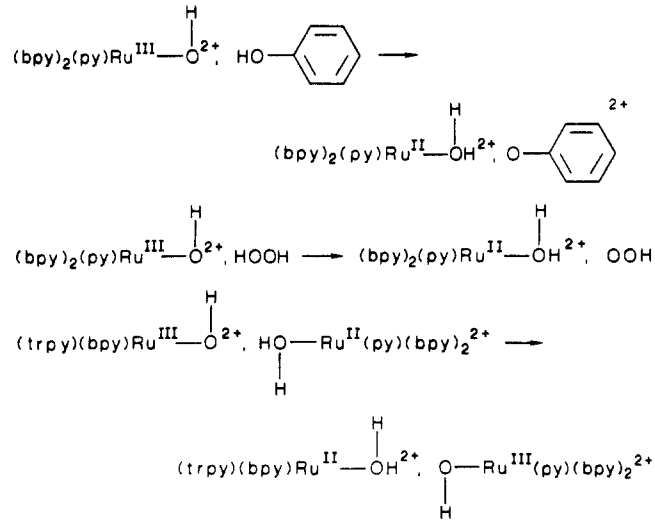

bifunctional in that it involves both the hydroxo group and the metal. In that sense, a more adequate description of the redox step is that it involves "proton-coupled electron transfer" rather than H atom transfer. Electron flow occurs from the π, σ, or d_π orbitals of C_6H_5OH, H_2O_2, or $[(bpy)_2(py)Ru^{II}(H_2O)]^{2+}$ to the vacancy in the $(d_\pi)^5$ core of the metal with concomitant transfer of the proton from the reductant to the O atom of the hydroxo group.

Oxidation by $Ru^{IV}=O^{2+}$. The key feature in the oxidation of phenols by $[(bpy)_2(py)Ru^{IV}(O)]^{2+}$ is the quantitative appearance of the quinone intermediates. The initial redox step leads to the 2e hydroquinone complex (eq 3). Its formation includes contributions from both preassociation and the actual redox step (eq 12 and 13). In eq 12, K_A is the preassociation constant between reactants. k_{red} is the rate constant for the redox step. It is defined as $k_{red} = (k_{obs}/2)/K_A$. Direct evidence for the preassociation step appears at high concentrations of phenol in the plot of k_{obs} vs [PhOH] in Figure 6. The generalized rate law for the mechanism described by reactions 12 and 13 is given by eq 14.[31] In eq 14

(28) (a) Zombeck, A.; Drago, R. S.; Corden, B. B.; Gaul, J. H. *J. Am. Chem. Soc.* **1981**, *103*, 7580. (b) Bedell, S. A.; Martell, A. E. *Inorg. Chem.* **1983**, *22*, 364. (c) Capdevielle, P.; Maumy, M. *Tetrahedron Lett.* **1983**, *24*, 5611.

(29) Forrester, A. R.; Thompson, R. H. *J. Chem. Soc. C* **1966**, 1844.

(30) Teuber, H. J.; Dietz, K. H. *Angew. Chem., Int. Ed. Engl.* **1965**, *4*, 871.

(31) Espenson, J. H. *Chemical Kinetics & Reaction Mechanisms*; McGraw-Hill: New York, 1981; p 104.

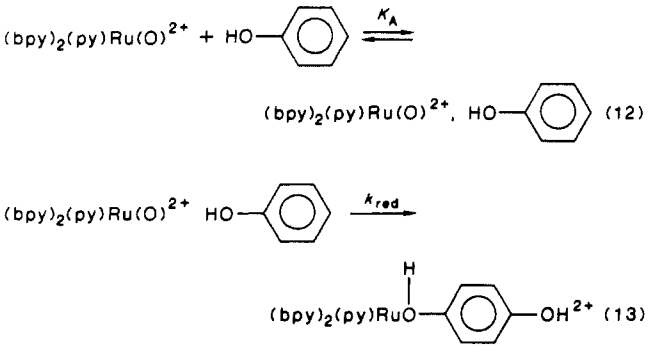

$$-d[Ru^{IV}{=}O^{2+}]/dt = \{2k_{red}K_A[PhOH]/(K_A[PhOH] + 1)\}[Ru^{IV}{=}O^{2+}]_{total} \quad (14)$$

$[Ru^{IV}{=}O^{2+}]_{total}$ is the total concentration of $Ru^{IV}{=}O^{2+}$ both free and present in the association complex with phenol. Under pseudo-first-order conditions in phenol the observed rate constant for the reaction, k_{obs}, is given by eq 15. From the slopes and

$$1/(k_{obs}/2) = 1/k_{red} + 1/k_{red}K_A[PhOH] \quad (15)$$

intercepts of the inverse–inverse plots suggested by eq 15 (Figure 6), at 25 °C, $k_{red} = 5.6\ s^{-1}$, $K_A = 3.3\ M^{-1}$ in CH_3CN and $k_{red} = 16.6\ s^{-1}$, $K_A = 3.6\ M^{-1}$ in H_2O.

It is possible to estimate K_A independently from the statistically derived Eigen–Fuoss equation[32]

$$K_A = 4\pi N_0(a_1 + a_2)^3/3000$$

This equation assumes that the reactants can be treated as spheres of radii a_1 and a_2. With $a_{Ru} = 6.2$ Å and $a_{PhOH} = 3.5$ Å, $K_A = 2.4$, which is within experimental error of the values obtained in the kinetic studies. The calculation shows that there is no need to invoke a special affinity between $Ru^{IV}{=}O^{2+}$ and phenol. In a statistical sense, at high concentrations of phenol, there is a high probability of finding a phenol molecule in the outer coordination sphere of the oxidant.

In terms of a mechanistic analysis, there is an additional contributing factor in the redox step that appears in k_{red}. Past preassociation of the reactants, there is a requirement that the oxidant and reductant be oriented in specific ways. Oxo attack on the aromatic ring requires that only certain specific relative orientations within the association complex can be productive in a mechanistic sense, e.g.

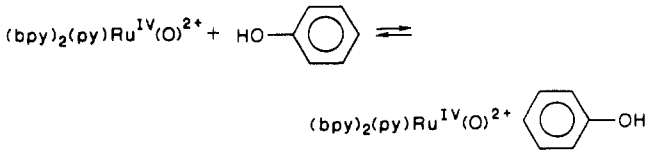

Evidence concerning the nature of the actual redox step is available from the magnitudes of k_{CH}/k_{CD} and k_{OH}/k_{OD} kinetic isotope effects, the ^{18}O-labeling result, the rate enhancements for alkyl-substituted phenols, and the rate enhancement of $>10^6$ in CH_3CN for PhOH compared to PhOMe.

As for $[(bpy)_2(py)Ru^{III}(OH)]^{2+}$, $[(bpy)_2(py)Ru^{IV}(O)]^{2+}$ is a moderately strong oxidant (Scheme I), but it does have the capacity to act as either a 2e oxidant via the Ru(IV/II) couple or a 1e oxidant via the Ru(III/II) couple.[6,7,8c,18] The existence of possible 2e pathways increases the mechanistic possibilities.

The k_{CH}/k_{CD} kinetic isotope effect of 6.3 observed in CH_3CN is consistent with an initial H atom transfer step like that proposed for Ru^{III}—OH^{2+} in CH_3CN. If H atom transfer does occur the intermediate 1e products must undergo a further redox reaction with Ru^{III}—OH^{2+} attack on the ring, before they separate through the surrounding solvent cage. This conclusion is demanded by the quantitative appearance of the Ru^{II}–quinone intermediate as the initial product. It follows from Scheme III that if the 1e

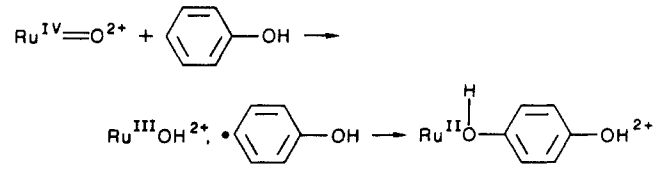

products separate in solution, a distribution of outer-sphere and inner-sphere products must be observed. The same demands would be placed on initial proton-coupled electron transfer from the O atom of phenol.

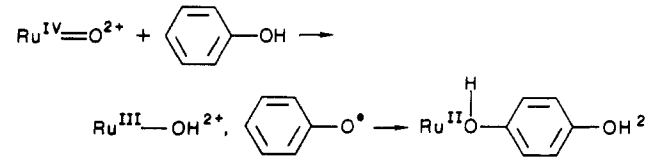

There is clear precedence for $Ru^{IV}{=}O^{2+}$ acting as a 2e oxidant with oxo atom transfer to the reductant.[7] The O atom transfer reactivity suggests an electrophilic character at the oxo group. The electrophilic character is a shared property of the metal–oxo combination. In an electronic sense, the acceptor orbitals are largely $d_\pi(Ru)$ in character (t_{2g} in O_h symmetry). The metal-based acceptor orbitals are strongly mixed with oxygen p orbitals, which promote the Ru–oxo interaction. From temperature-dependent magnetic studies,[20b] the ground electronic state has the configuration $(d_{\pi_1})^2(d_{\pi_2})^2(d_{\pi_3})^0$ with a low-lying, thermally accessible magnetic state of configuration $(d_{\pi_1})^2(d_{\pi_2})^1(d_{\pi_3})^1$. In an electronic sense, the O atom of the oxo group can be viewed as a "lead in" atom, with the electrophilic character and net electron flow occurring to the vacancies in the d_π levels.

Given the electrophilic character of $Ru^{IV}{=}O^{2+}$, an alternate mechanistic possibility is direct electrophilic attack on the aromatic ring. A related pathway has been demonstrated in the oxidative,

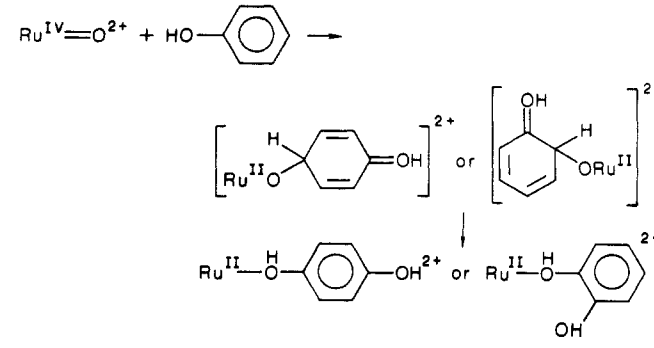

electrophilic attack by Br_2 on phenols at low temperature. The reactions occur via direct Br^+ attack on the aromatic ring[33] as

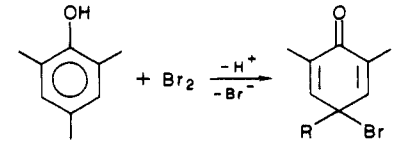

demonstrated by the appearance of the Br addition product when R is an allyl. Electrophilic attack on phenol by NO_2^+ has also been invoked in the nitration of phenol by dilute HNO_3.[34]

On the basis of the results of many mechanistic studies, it has been concluded that an important, general pathway for electrophilic addition to aromatics in via initial attack and intermediate formation. The reactions are completed by subsequent loss of H^+ to an added base or to the solvent[33,35] (eq 16). The bonding in

$$Ar + E^+ \underset{k_{-1}}{\overset{k_1}{\rightleftharpoons}} Ar\cdots E^+ \xrightarrow[k_2]{-H^+} ArE + H^+ \quad (16)$$

(32) (a) Fuoss, R. M. *J. Am. Chem. Soc.* **1958**, *80*, 5059. (b) Sutin, N. *Prog. Inorg. Chem.* **1983**, *30*, 441.

(33) (a) March, J. *Advanced Organic Chemistry*; McGraw-Hill: New York, 1977; p 453. (b) Lowry, T. H.; Richardson, K. S. *Mechanism & Theory in Organic Chemistry*; Harper & Row: New York, 1987; pp 623–624.

(34) Schofield, K. *Aromatic Nitration*; Cambridge University: London, 1981.

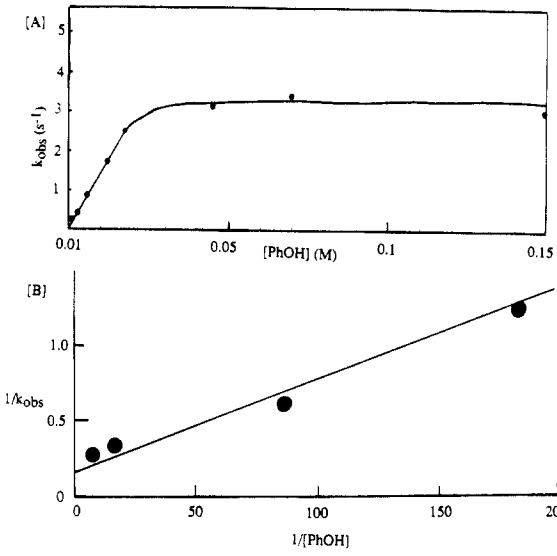

Figure 6. Plot of k_{obs} vs [PhOH] (A) and the inverse–inverse plot (B) for the reaction between $[(bpy)_2(py)Ru(O)]^{2+}$ and phenol in CH_3CN at 25.0 (±0.1) °C.

the intermediate Ar···E^+ may involve π complexation to the ring or to an isolated double bond in the ring or σ complexation as in the case of Br^+. From kinetic studies on electrophilic addition, many examples have been identified where the rate-determining step is adduct formation.[36] In this limit k_{CH}/k_{CD} is small as might have been expected. However, for the electrophilic addition of *p*-chlorobenzenediazonium ion to sulfonate-substituted phenoxides in water, a reasonably large kinetic isotope effect (6.55) is observed.[37] The suggestion was made that for these reactions a significant contribution in a rate-determining sense comes from the proton loss step in eq 16. With added pyridine as a base, the isotope effect fell to an intermediate value, suggesting that, under those conditions, the k_1 and k_2 steps in eq 16 are comparable ratewise.[38]

If the $Ru^{IV}{=}O^{2+}$ oxidation proceeds via electrophilic attack on phenol (Scheme IV), a situation may exist where electrophilic attack and subsequent CH-based H^+ transfer to $-ORu^{II}$ are also nearly competitive ratewise. Such a competition would explain the apparent change in mechanism between water and acetonitrile. The change in mechanism is signaled by the differences in activation parameters, $\Delta H^{\ddagger} = 10.3 \pm 0.6$ kcal/mol, $\Delta S^{\ddagger} = -14 \pm 2$ eu, in CH_3CN, and $\Delta H^{\ddagger} = 6.4 \pm 1.5$ kcal/mol, $\Delta S^{\ddagger} = -24 \pm 4$ eu, in H_2O,[39] and by the loss of the k_{CH}/k_{CD} isotope effect in H_2O, Table VI. The sizable CH kinetic isotope effect of $k_{CH}/k_{CD} = 5.5$ in CH_3CN suggests rate-limiting C–H bond breaking by H^+ loss (k_2) after initial electrophilic attack (k_1). The loss of a CH-based kinetic isotope effect in water suggests that, in H_2O, initial electrophilic attack is rate limiting. The change in rate-determining steps between CH_3CN and H_2O is not surprising

Scheme IV

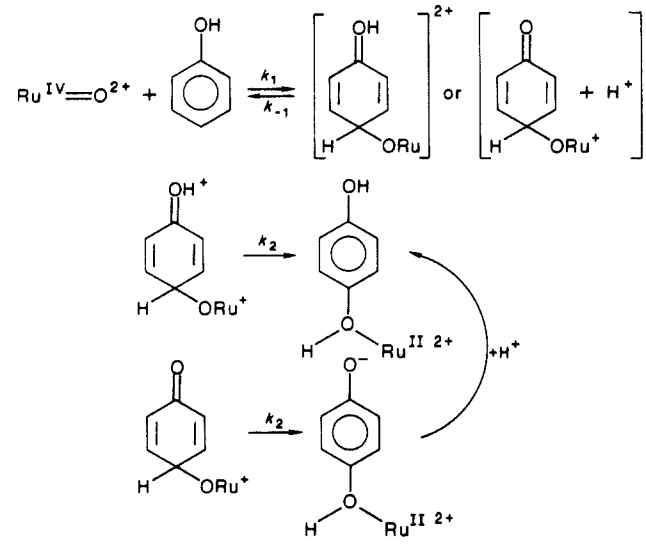

given the much greater ability of H_2O to act as a base for the H^+ released from the C–H bond.

A slightly altered mechanism is also shown in Scheme IV in which OH-based H^+ loss occurs concomitantly with electrophilic attack. It would help to explain both the considerable rate enhancement for phenol compared to anisole and the origin of the OH kinetic isotope effect, $k(H_2O)/k(D_2O) = 3.5$. The acceleration in rate above pH 7 could also be accounted for by this mechanism rather than by invoking a pathway involving the phenoxide ion.

Acknowledgment is made to the National Science Foundation under Grant No. CHE-8601604 for support of this research.

Registry No. 1, 116374-43-7; **2**, 116374-44-8; **5**, 116374-56-2; [Ru(bpy)$_2$(CO_3)], 59460-48-9; $[(bpy)_2(py)Ru^{II}(CH_3CN)]^{2+}$, 82769-09-3; $[(bpy)_2(py)Ru(OH)]^{2+}$, 75495-07-7; $[(bpy)_2(py)Ru^{IV}{=}O]^{2+}$, 67202-43-1; D_2, 7782-39-0; phenol, 108-95-2; *p-tert*-butylphenol, 98-54-4; *p*-phenylphenol, 92-69-3; *o*-cresol, 95-48-7; *p*-cresol, 106-44-5; *o*-isopropylphenol, 88-69-7; 2,6-dimethylphenol, 576-26-1; 3,5-dimethylphenol, 108-68-9; 2,3-dimethylphenol, 526-75-0; 2,3,6-trimethylphenol, 2416-94-6; *o*-benzoquinone, 583-63-1; *p*-benzoquinone, 106-51-4; 4-*tert*-butyl-1,2-benzoquinone, 1129-21-1; 4-phenyl-1,2-benzoquinone, 17189-95-6; 6-methyl-1,2-benzoquinone, 4847-64-7; 2-methyl-1,4-benzoquinone, 553-97-9; 4-methyl-1,2-benzoquinone, 3131-54-2; 6-isopropyl-1,2-benzoquinone, 98353-93-6; 2-isopropyl-1,4-benzoquinone, 15232-10-7; 2,6-dimethyl-1,4-benzoquinone, 527-61-7; 3,5-dimethyl-1,2-benzoquinone, 4370-49-4; 3,4-dimethyl-1,2-benzoquinone, 4542-65-8; 2,3-dimethyl-1,4-benzoquinone, 526-86-3; 2,3,6-trimethyl-1,4-benzoquinone, 935-92-2; (4-*tert*-butyl-1,2-benzoquinone)bis(2,2′-bipyridine)pyridineruthenium(2+), 116374-45-9; (4-phenyl-1,2-benzoquinone)bis(2,2′-bipyridine)pyridineruthenium(2+), 116374-46-0; (3-methyl-1,2-benzoquinone)bis(2,2′-bipyridine)pyridineruthenium(2+), 116374-47-1; (4-methyl-1,2-benzoquinone)bis(2,2′-bipyridine)pyridineruthenium(2+), 116374-48-2; (3-isopropyl-1,2-benzoquinone)bis(2,2′-bipyridine)-pyridineruthenium(2+), 116374-49-3; (2,6-dimethyl-1,4-benzoquinone)bis(2,2′-bipyridine)pyridineruthenium(2+), 116374-50-6; (3,5-dimethyl-1,2-benzoquinone)bis(2,2′-bipyridine)pyridineruthenium(2+), 116374-51-7; (3,4-dimethyl-1,2-benzoquinone)bis(2,2′-bipyridine)-pyridineruthenium(2+), 116374-52-8; (2,3,6-trimethyl-1,4-benzoquinone)bis(2,2′-bipyridine)pyridineruthenium(2+), 116374-53-9; (1,2-benzoquinone)bis(2,2′-bipyridine)pyridineruthenium(2+), 116374-54-0; (2-methyl-1,4-benzoquinone)bis(2,2′-bipyridineruthenium(2+), 116405-36-8; (2-isopropyl-1,4-benzoquinone)bis(2,2′-bipyridineruthenium(2+), 116374-55-1; (2,3-dimethyl-1,4-benzoquinone)bis(2,2′-bipyridine-ruthenium(2+), 116374-57-3.

(35) Melander, L. *Ark. Kemi* **1950**, *2*, 211.
(36) (a) Zollinger, H. *Adv. Phys. Org. Chem.* **1964**, *2*, 163. (b) Berliner, E. *Prog. Phys. Org. Chem.* **1964**, *2*, 253.
(37) (a) Zollinger, H. *Helv. Chim. Acta* **1955**, *38*, 1597, 1623. (b) Ernst, R.; Sramm, O. A.; Zollinger, H. *Helv. Chim. Acta* **1958**, *41*, 2274.
(38) de la Mare, P. B. D. *Electrophilic Halogenation*; Cambridge University: London, 1976.
(39) The activation parameters for H_2O at pH 7 include a small contribution from the k_{OH^-} term in eq 9 (Table V), which complicates any detailed comparisons.